Effects of vacuum ultraviolet and ultraviolet irradiation on ultrathin hafnium-oxide dielectric layers on (100)Si as measured with electron-spin resonance

H. Ren,[1] S. L. Cheng,[2] Y. Nishi,[2] and J. L. Shohet[1,a)]
[1]Department of Electrical and Computer Engineering, Plasma Processing and Technology Laboratory, University of Wisconsin–Madison, Madison, Wisconsin 53706, USA
[2]Stanford University, Stanford, California 94305, USA

(Received 25 March 2010; accepted 27 April 2010; published online 14 May 2010)

The effects of vacuum ultraviolet (VUV) (7.2 eV) and UV (4.9 eV) irradiation on hafnium-oxide dielectric layers were studied with electron-spin resonance to detect defect states. Silicon dangling-bond defects (P_b centers) and positively charged oxygen vacancies (E' centers) were detected with g-factor fitting. VUV irradiation increases the level of P_b states, while UV decreases the level of P_b states but increases the level of E' states significantly. Rapid thermal annealing appears to mitigate these effects. Absolute values of the defect-state concentrations are presented.
© 2010 American Institute of Physics. [doi:10.1063/1.3430570]

During plasma processing of microelectronic devices, dielectrics are exposed to vacuum ultraviolet (VUV) and UV radiation.[1,2] This can modify the number of defect states in the dielectric.[3,4] Electron-spin resonance (ESR) detects those defect states that have paramagnetic electrons.[5,6] Hafnium oxide (HfO_2) is a well-known high-k dielectric material and is a potential gate dielectric for complementary metal oxide semiconductor devices.[7] Previous work using ESR shows that HfO_2 has numerous defect states.[8–11] The most common are P_{b0}, P_{b1}, E', EX, etc. The EX defect state, which is the positively charged bulk-oxide defect state, appears during the growth or modification of SiO_2-like interfacial layers.[5] Since no modifications were made to the interfacial layers, we only examine the P_{b0}, P_{b1}, and E' states.

In this letter, we utilize ESR to examine the effects of VUV and UV irradiation[12] on room-temperature-atomic-layer-deposited 20-nm-thick HfO_2 on (100)Si. The resistivity of the silicon substrate is 4000 Ω cm which is needed to obtain ESR measurements.[13] The HfO_2 wafers were rapid thermally annealed (RTA) at 800 °C. A comparison between as-deposited and RTA samples was made. Each sample was prepared with an area of 10×2 mm^2. Seven samples were used in order to maximize the signal.

To obtain the g-factors and levels for the observed defect states, we assume that the ESR signal is the sum of contributions from each of the defect states. Each defect state varies with the external magnetic field B and has the form of the derivative of a Gaussian as

$$I_i(B) = -\frac{2A_{i0}(B-B_{i0})}{\sigma_i^2}e^{-(B-B_{i0})^2/\sigma_i^2} \quad (1)$$

where A_{i0}, B_{i0}, and σ_i are found during the least-squares fitting process. A_{i0} is the amplitude, σ_i is the B-field width of the defect state, and B_{i0} allows us to determine the g-factor of the defect state with the expression[14]

$$g_i = \frac{h\nu}{\mu_B B_{i0}}, \quad (2)$$

where h is Planck's constant, μ_B is the Bohr magneton $eh/(4\pi m_e)$, and ν is the frequency of the oscillating magnetic field.

The relative concentration of each defect state is calculated using the following expression:

$$C_{ir} = \int_{B_{\rm low}}^{B_{\rm high}}\int_{B_{\rm low}}^{B_{\rm high}} I_i(B)dBdB \approx \sqrt{\pi}A_{i0}\sigma_i, \quad (3)$$

where C_{ir} is the relative concentration for the defect state i. $B_{\rm low}$ and $B_{\rm high}$ are the minimum and maximum values of the scanned magnetic field. The inner integral recovers the original signal as a Gaussian while the outer integral calculates the level of defect states for that particular Gaussian. The concentrations of the defect states are linearly dependent on the intensity A_{i0} and the standard deviation σ_i (B-field width) of the signal. With Eqs. (2) and (3), both the g-factors and the absolute values of the levels of the defect states can be found.

To identify the P_{b0}, P_{b1}, and E' defect states, ESR measurements were made on unexposed samples as a function of magnetic field orientation.[5,15] At $\theta=0$ (B-field parallel to the sample normal), the P_{b0}, P_{b1}, and E' states were found with g-factors of 2.0062, 2.0037, and 2.0002, respectively. These are typical values for the corresponding g-factors of the defect states.[5,16]

Next, as-deposited and RTA HfO_2 samples were exposed to VUV at the UW-Madison synchrotron. The beam energy was 7.2 eV which is above the band gap of HfO_2. In addition, an absorption peak, measured with VUV spectroscopy, occurs at this energy.[17] The photon dose was approximately 5.4×10^{14} photons/cm^2.

Following VUV exposure, ESR measurements were made with the B-field parallel to the surface normal of the sample. The measured and fit ESR signals for both unexposed and VUV-exposed samples are shown as curves (a) and (b) in Fig. 1. The corresponding concentrations of the defect states are presented in Table I. Table I shows that the

a)Electronic mail: shohet@engr.wisc.edu.

Author complimentary copy. Redistribution subject to AIP license or copyright, see http://apl.aip.org/apl/copyright.jsp

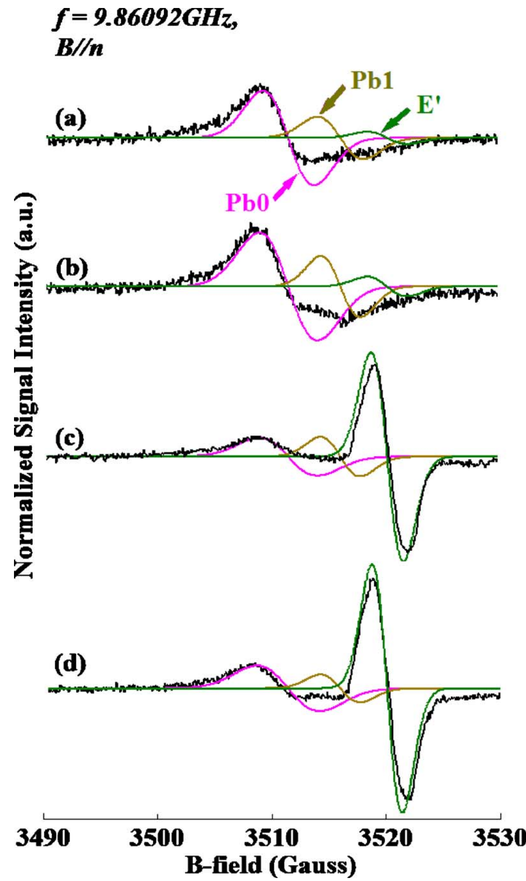

FIG. 1. (Color online) Selected ESR signals and defect-state fitting curves: B-field direction parallel to surface normal of the as-deposited samples. (a) No treatment. (b) After 7.2 eV VUV exposure. (c) After 4.9 eV UV exposure. (d) VUV+UV exposure. The g-factors for P_{b0}, P_{b1}, and E' states in this case are 2.0062, 2.0037, and 2.0002, respectively.

P_{b0}, P_{b1}, and E' levels all increase after VUV irradiation. The P_{b0} and P_{b1} concentrations of the as-deposited samples both increased (16.7% and 2.5%, respectively) while the E' concentration was one order of magnitude smaller.

Table I shows that after VUV exposure of the RTA sample, the levels of the defect states increased by smaller amounts. We can see that the concentrations of the unexposed and VUV-exposed RTA samples are always lower than the as-deposited samples. Therefore, RTA decreases the defect-state concentrations before irradiation and minimizes their increase during irradiation.

We now turn to UV exposure. First, a 4.9 eV UV exposure was made on an as-deposited HfO_2 sample for 2 min using a mercury lamp. Compared to an unexposed sample, the UV-irradiated sample showed the following differences in the defect state concentrations. The P_{b0} and P_{b1} state concentrations decreased by 26% and 0.5%, respectively. UV *increased* the E' state concentration *significantly* from 8.81×10^{10} to 1.42×10^{12} cm^{-2}. The corresponding ESR signals are shown in curve (c) of Fig. 1.

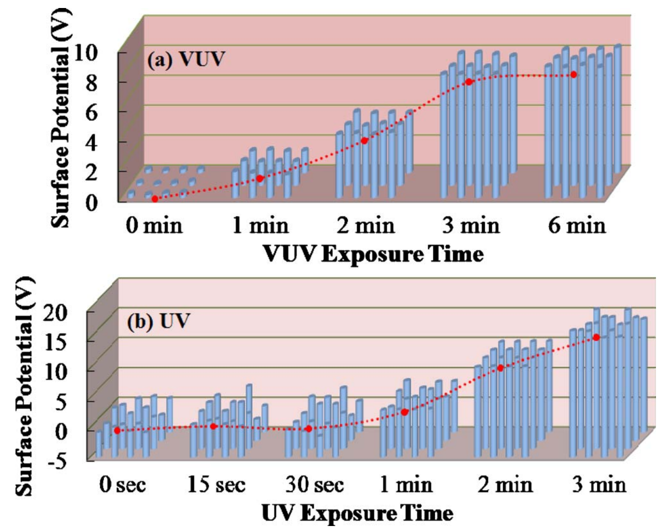

FIG. 2. (Color online) Surface potential as a function of VUV and UV irradiation time. (a) Surface potential with VUV exposure. (b) Surface potential with UV exposure.

Following this, a UV exposure was made on an RTA HfO_2 sample for 2 min. The P_{b0} and P_{b1} state concentrations decreased by 7.9% and 12.6%, respectively. The E' state concentration continued to show a significant increase from 4.79×10^{10} to 4.28×10^{11} cm^{-2}.

Finally, a combination of VUV and UV exposures was made. First, after VUV exposure, the as-deposited HfO_2 was irradiated with a 4.9 eV mercury lamp for three minutes. The ESR measurements are shown in curve (d) of Fig. 1. The P_b state concentrations decreased slightly. However, the E' state levels still increased significantly from 1.23×10^{11} to 2.65×10^{12} cm^{-2}. The same results were seen when the RTA sample was exposed to both VUV and UV. Reversing the order of the VUV and UV irradiation showed no difference in the observed defect-state levels.

To determine the reasons for this, Kelvin probe surface-potential measurements were made. The surface potential of the as-deposited HfO_2 was measured as shown in Fig. 2(a). Before VUV exposure, the surface potential was close to zero. During VUV, the surface potential increased and saturated at 10 V. This is believed to be due to the depletion of electrons during VUV irradiation.[4] Before VUV irradiation, the P_b-type defect states are filled with electrons. The electrons are depleted by photoemission and positive-charge trapping during irradiation. Since the band gap for HfO_2 is

TABLE I. Absolute values of the defect-state concentrations.

Concentration (cm^{-2})		No treatment	VUV only	UV only	VUV+UV	UV+VUV
As-deposited	P_{b0}	1.14×10^{12}	1.33×10^{12}	8.43×10^{11}	1.25×10^{12}	1.21×10^{12}
	P_{b1}	4.07×10^{11}	4.17×10^{11}	4.05×10^{11}	4.00×10^{11}	4.08×10^{11}
	E'	8.81×10^{10}	1.23×10^{11}	1.42×10^{12}	2.65×10^{12}	2.44×10^{12}
RTA	P_{b0}	8.26×10^{11}	8.85×10^{11}	7.61×10^{11}	8.11×10^{11}	8.73×10^{11}
	P_{b1}	3.88×10^{11}	4.01×10^{11}	3.39×10^{11}	3.50×10^{11}	3.92×10^{11}
	E'	4.79×10^{10}	5.33×10^{10}	4.28×10^{11}	5.66×10^{11}	4.97×10^{11}

Author complimentary copy. Redistribution subject to AIP license or copyright, see http://apl.aip.org/apl/copyright.jsp

around 5.7 eV,[18,19] the 7.2 eV photons generate electron photoemission which leads to positive charge accumulation on the sample surface.

For UV irradiation, the E' defect level increases significantly. These oxygen-vacancy defects can easily transfer electrons into the silicon,[19] resulting in an increase in the surface potential. On the other hand, some of the electrons generated from photoinjection from the substrate are trapped in the P_b states so that the P_b-state concentration levels decrease, resulting in a decrease in surface potential. As a result, the surface potential during UV exposure depends on the relative magnitudes these two opposing effects.

Figure 2(b) shows the surface potential as a function of time during UV exposure. During the initial minute of UV exposure, the creation and depopulation of the E' defect states counteracts the repopulation of the P_b states, keeping the surface potential relatively constant. After this, the P_b states are repopulated with electrons while the E' state levels keep increasing. This leads to the measured surface-potential increase.

Because the band gap of the E' state is around 4 eV,[19,20] the 4.9 eV photons are quite likely to increase the E' defect levels. The effects of photoemission are negligible, since the UV photon energy is below the HfO_2 band gap (5.7 eV). However, photoinjection of electrons does happen and neutralizes some of the positive charges at the interfacial layer and helps repopulate the electrons in P_b-type states. Because the HfO_2 layer is ultrathin and the UV photon energy is below the band gap, trap-assisted tunneling may also take place,[21] which can contribute to the positive surface potential.

In conclusion, we find that VUV irradiation increases the P_b defect levels in ultrathin HfO_2 due to electron depletion from the defects.[17] The depletion takes place because photoemission and positive-charge trapping occur when the incident VUV photon energy is larger than the band gap resulting in a positive surface potential. Then, UV irradiation can decrease the P_b defect levels by electron repopulation of the defects. The electrons come from photoinjection of electrons from the silicon substrate and/or electron transfer from oxygen vacancies resulting in a decrease in the surface potential. However, 4.9 eV UV irradiation increases the E' defect levels significantly. This overcomes the effect of the P_b-state decrease and results in an overall positive surface potential.

We thank M. Ivancic for helping set up the ESR experiments. This work is supported by the Semiconductor Research Corporation under Contract No. 2008-KJ-1781. The UW Synchrotron is supported by NSF Grant No. DMR-0084402.

[1] J. R. Woodworth, M. G. Blain, R. L. Jarecki, T. W. Hamiliton, and B. P. Aragon, J. Vac. Sci. Technol. A **17**, 3209 (1999).
[2] C. Cismaru and J. L. Shohet, Appl. Phys. Lett. **74**, 2599 (1999).
[3] G. S. Upadhyaya, J. L. Shohet, and J. L. Lauer, Appl. Phys. Lett. **86**, 102101 (2005).
[4] J. L. Lauer, H. Sinha, M. T. Nichols, G. A. Antonelli, Y. Nishi, and J. L. Shohet, "Charge trapping within UV and VUV irradiated low-*k* porous organosilicate dielectrics," J. Electrochem. Soc. (to be published).
[5] B. B. Triplett, P. T. Chen, Y. Nishi, P. H. Kasai, J. J. Chambers, and L. Colombo, J. Appl. Phys. **101**, 013703 (2007).
[6] A. Stesmans and V. V. Afanas'ev, Appl. Phys. Lett. **85**, 3792 (2004).
[7] G. D. Wilk, R. W. Wallace, and J. M. Anthony, J. Appl. Phys. **89**, 5243 (2001).
[8] Y. Nishi, Jpn. J. Appl. Phys. **10**, 52 (1971).
[9] A. Stesmans and V. V. Afanas'ev, J. Appl. Phys. **97**, 033510 (2005).
[10] E. H. Poindexter, P. J. Caplan, B. E. Deal, and R. R. Razouk, J. Appl. Phys. **52**, 879 (1981).
[11] E. P. O'Reilly and J. Robertson, Phys. Rev. B **27**, 3780 (1983).
[12] C. P. Poole and H. A. Farach, *ASM Handbook*, (ASM International, Materials Park, Ohio, 1986), Vol. 10, pp. 253–266.
[13] M. Tabib-Azar, D. Akinwande, G. E. Ponchak, and S. R. LeClair, Rev. Sci. Instrum. **70**, 3083 (1999).
[14] A. Schweiger and G. Jeschke, *Principles of Pulse Electron Paramagnetic Resonance* (Oxford University Press, Oxford, 2001).
[15] G. W. Ludwig and H. H. Woodbury, Phys. Rev. **113**, 1014 (1959).
[16] G. Buscarino and S. Agnello, J. Non-Cryst. Solids **353**, 577 (2007).
[17] J. L. Lauer, J. L. Shohet, and Y. Nishi, Appl. Phys. Lett. **94**, 162907 (2009).
[18] N. V. Nguyen, A. B. Davydov, D. Chandler-Horowitz, and M. M. Frank, Appl. Phys. Lett. **87**, 192903 (2005).
[19] K. Xiong, J. Robertson, M. C. Gibson, and S. J. Clark, Appl. Phys. Lett. **87**, 183505 (2005).
[20] P. Broqvist and A. Pasquarello, Appl. Phys. Lett. **90**, 082907 (2007).
[21] M. Houssa, M. Tuominen, M. Naili, V. Afanas'ev, A. Stesmans, S. Haukka, and M. M. Heyns, J. Appl. Phys. **87**, 8615 (2000).

Author complimentary copy. Redistribution subject to AIP license or copyright, see http://apl.aip.org/apl/copyright.jsp